A simple method to estimate the airfoil maximum drag coefficient

Timmer, W. A.

DOI
10.1088/1742-6596/1618/5/052068

Publication date
2020

Document Version
Final published version

Published in
Journal of Physics: Conference Series

A simple method to estimate the airfoil maximum drag coefficient

A simple method to estimate the airfoil maximum drag coefficient

W.A.Timmer

Department of Aerodynamics, Wind Energy and Flight Performance and Propulsion

Faculty of Aerospace Engineering

Delft University of Technology, The Netherlands

Contact: w.a.timmer@tudelft.nl

Keywords: airfoil performance, deep stall, maximum drag coefficient, blockage, wall corrections

Abstract

A relatively simple method is presented to predict the maximum two-dimensional drag coefficient of an airfoil only using its shape. The method is based on a contribution related to the leading edge thickness in terms of the y/c coordinate at x/c=0.0125 and a contribution related to the trailing edge flow angle which appears also to be sensitive to the leading edge thickness. The relations were deduced from measurements in the Delft low-turbulence wind tunnel. The first contribution was established using 3 airfoil models with systematically varying leading edge y/c coordinates and a zero trailing edge angle. The second followed from measurements of one of these airfoils equipped with sheet metal flaps of various flap deflections. Compared to measurements found in the public domain differences are found up to $\pm$ 2.3% with an average of about -0.2%

1. Introduction

During wind turbine starts and stops of both vertical axis and horizontal axis wind turbines and during blade hoisting the angle of attack of rotor blades can reach very high values, and the maximum drag force for positive as well as negative angles may play a role in the loads, which partly may be traced back to the airfoils in the blade.

In literature a number of experiments can be found dealing with the performance of airfoils over the entire 360 degrees range of angles of attack, [1]-[7]. Although the list is growing, still there's no abundant amount of data available. As test setup, model accuracy, data reduction and applied wind tunnel blockage correction schemes differ quite a bit in the various available publications, or have not been sufficiently described, it is sometimes difficult to extract the most essential information in a direct fashion. Moreover, the heavily fluctuating forces in the deep stall region give rise to large data scatter, increasing uncertainties and making the performance characteristics heavily depending on averaging times. This results in the fact that measured aerodynamic characteristics for the same airfoil sometimes do not match well.

Although the dynamics of the flow play an important role in the instantaneous forces, with sufficient averaging time it is possible to extract some sort of two-dimensional characteristic for a particular airfoil. Since for large positive angles of attack the entire upper surface is separated from the leading edge (LE), the downwind shape of the airfoil does not play a role in the drag force, provided that the airfoil upper surface thickness does not protrude deep into the wake where the motion of the vortex

street behind the airfoil will be affected. Generally the airfoil has a relatively sharp trailing edge (TE), which leads to immediate separation. This leaves the lower surface leading edge as a major contributor to differences in airfoil maximum drag, as only the leading edge flow can impact the width of the wake and the separation location and associated pressure (which determines the base pressure). The same goes mutate mutandis for large negative angles. In [8] it is shown that with increasing leading edge thickness the maximum drag coefficient of airfoils decreases. The thickness of the LE was defined as the y/c value of the upwind part of the airfoil leading edge at x/c=0.0125. Also in the present study the results are based on this leading edge coordinate. Though quite arbitrary (it could very well be x/c=.005, .01, or the dy/dx at one of the x-stations at the leading edge) the value of x/c=0.0125 worked well for the onset of deep-stall of airfoils published in [8], which followed the work of Gault [9], who used it for typifying airfoil stall. The leading edge cannot be represented by the nose radius, as there is only one, while for negative and positive angles the maximum drag coefficient for non-symmetrical airfoils differs. Apart from the thickness at the leading edge, the angle at which the flow leaves the trailing edge (ζ) when the chord is normal to the flow can be identified as a key parameter. The present study aims at quantifying the contribution to the maximum drag coefficient of both leading edge thickness and trailing edge angle.

2. The impact of the leading edge thickness

To be able to distinguish the contributions of the leading edge and the trailing edge to the total maximum drag a set of airfoil models with varying leading edge thickness and zero trailing edge angle (ζ=0) was designed and measured in the 1.25x1.80m low-speed low-turbulence tunnel (LTT) of Delft University. The airfoil shapes of the 0.2 m chord numerically milled aluminium models are depicted in figure 1. They have different elliptical leading edges for the upper and lower surfaces up to 34% of the chord, such that the 3 models cover the range of y/c values at x/c=0.0125 between .010 and .035. The last 20% of the airfoils are straight and the 4 mm thick trailing edges are sharp.

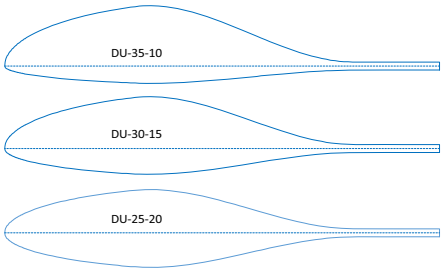

Figure 1: DU airfoils with prescribed upwind thickness at x/c=0.0125

2.1 Test setup and data handling.

The models were tested using the LTT 6-component external mechanical balance system. They were cantilevered from the overhead balance and were mounted normal to the flow. The angle of attack range departing from this position was +/- 45 degrees, being the maximum range of the balance system without re-orienting the model. The three models were tested first with the thicker upper surface pointing upwind (addressing angles of attack between -45 and -135 degrees), then rotated 180 degrees to test the model with the lower surface facing the incoming flow (incidences between 45 and 135 degrees). The 19% thick models (with comparable stiffness characteristics) completely spanned the 1.25m height of the tunnel, but leaving a gap of approximately 2.0 mm with the tunnel walls.

As the models were attached only at one end to the balance, to avoid heavy vibrations the Reynolds number was restricted to 0.45×10^6. The measured forces were recorded with 5 Hz and averaged over 40 seconds. In view of the strong dynamics in the flow the sampling time of 5Hz might seem very low, however due to the inertia of the balances (rotating spindles with running weights) strong fluctuations will not be followed, which already averages out large and fast variations effectively.

2.2 Blockage corrections

The high angles of attack and the large separated wake of the models lead to serious blockage of the wind tunnel test section, which increases the velocity over the model significantly and causes higher forces than in free air. To correct for the large overspeeds the method of Maskell [10] was followed, originally developed for bluff bodies. Maskell stated that it could also be used for two-dimensional bodies fully submerged in their own wake. The method accounts for the presence of the large wake and the distortion by the tunnel walls of the expansion of the wake. The corrections as given by Allen and Vincenti [11], often used to correct the measurements of two-dimensional airfoil characteristics are not suited for this type of flow, as their method is based on small perturbations from the main stream and does not account for the increasing impact of wake blockage on the flow. Maskell's corrected dynamic pressure for the case of a model with chord c spanning the tunnel width follows from

$$\frac{q_u}{q} = \frac{C_D}{C_{D_u}} = \frac{1}{1 + \theta \frac{c}{h} C_{D_u}} \tag{1}$$

The index u refers to the uncorrected properties and h is the effective tunnel height. The original formulation contains the uncorrected drag coefficient due to separation $C_{D,s}$. However, apart from the fact that this coefficient is hard to extract from the measurements, it seems justified to use the full uncorrected drag coefficient as for moderate blockages the difference especially when the flow is normal to the chord is usually in the order of 1% or less. The blockage parameter θ depends on model aspect ratio and is given to be 0.96 for two-dimensional configurations. For large values of c/h Maskell's method was found to over correct the drag coefficient, mostly for three-dimensional configurations [12]. Hackett and Cooper [13] extended Maskell's theory and divided the correction into a contribution due to the wake blockage and one due to the wake distortion. By removing the wake distortion for larger c/h values they claim to remove this tendency to over correct. Although their method seems to work remarkably well for some of the three-dimensional configurations they reviewed, the formulation of the method, as documented in [12] is unfortunately partly in error. For the present study it is assumed that for c/h values up to 0.15 equation 1 can be used without significant danger of over correction. The drag measurements presented here have a c/h value of 0.121 (a chord of 0.2m and an effective test section width of 1.656 m).

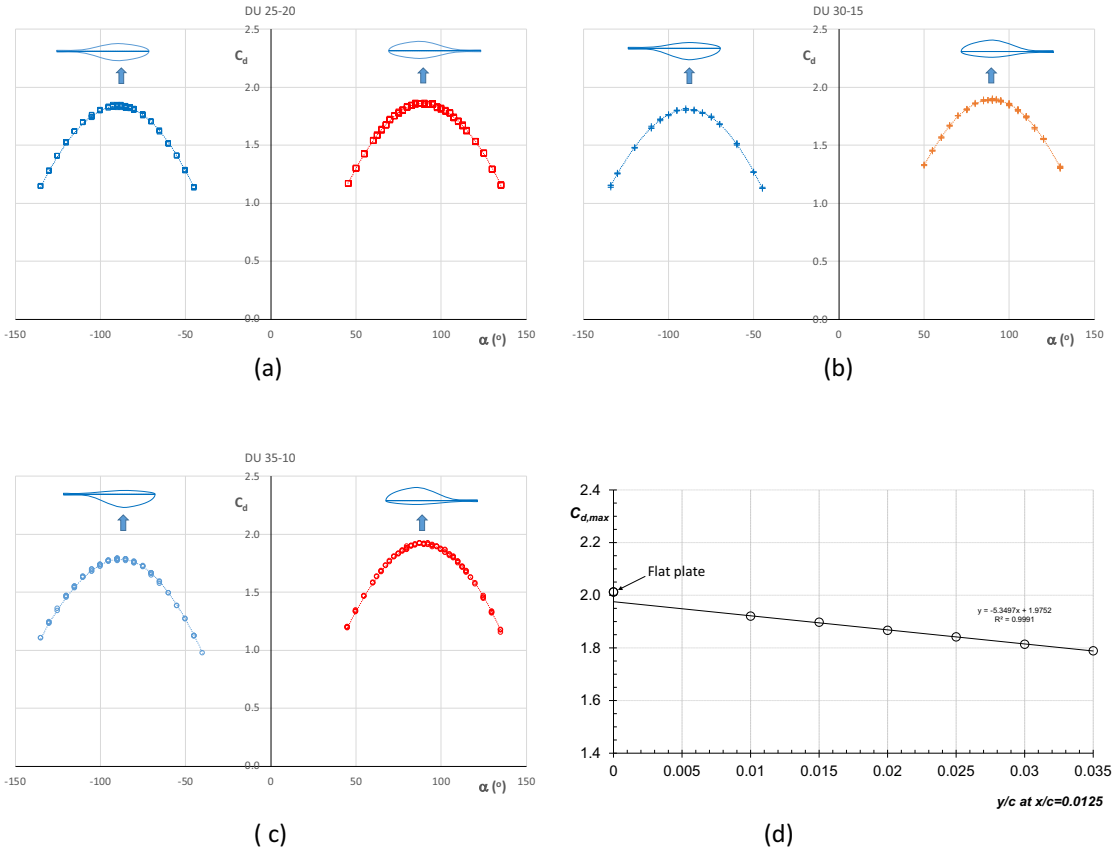

Figure 2: The measured and corrected drag coefficients for the 3 models depicted in figure 1.

2.3 Results

Figures 2a to 2c present the corrected drag measurements for all 6 configurations. The maximum drag coefficients shown in figure 2d and tabulated in table 1 were extracted from 6th degree polynomials through the measured points of the various models. The relation between the y/c at x/c=0.0125 and the maximum drag coefficient is found to be :

$$C_{d_{\max}} = 1.976 - 5.366 * (y/c)_{x/c=0.0125} \quad (2)$$

To show that the test yields near-two-dimensional drag coefficients also a flat plate was measured, giving a maximum drag coefficient of 2.012.

Table 1: The measured maximum drag coefficients deduced from the 6th degree polynomials

Airfoil	y/c	Cd -max	y/c	Cd -max
	positive angles		negative angles	
Flat plate	0	2.012		
DU-25-20	0.020	1.867	0.025	1.842
DU-30-15	0.015	1.898	0.03	1.814
DU-35-10	0.010	1.921	0.035	1.789

3. The effect of the trailing edge angle ζ

The flat plate and the model of DU 35-10 were also used to determine the impact of the trailing edge angle on the drag coefficient. To this end a number of 1 mm thick sheet metal flaps were manufactured with nominal angles of 0, 10, 15 and 20 degrees. The flaps were attached to the model as shown in figure 3.

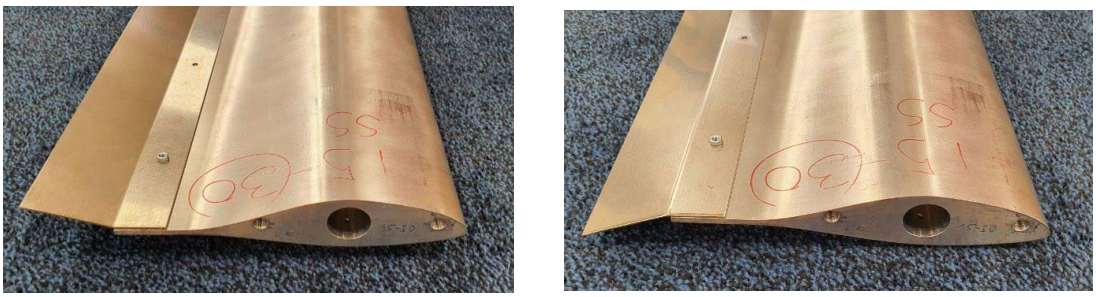

Figure 3: One of the DU models showing a 20 deg. negative (left) and positive (right) trailing edge (flap) angle when the airfoil faces the incoming flow with the thickest surface (negative angles).

The drag curves for the airfoil with flap were determined with 60 second averages of the force readings at a Reynolds number of $4*10^5$. Due to the elongation of the model the c/h value now has increased to 0.15. To determine the maximum drag coefficient the same procedure was followed as described above for the base airfoils.

Due to tunnel time constraint not all configurations were tested, however all the extreme values were covered. Figure 4 presents the measured values of the maximum drag coefficient in relation to the true trailing edge flow angle when the longest chord of the airfoil (the line between the trailing edge and the leading edge) is normal to the flow. The TE-angle is positive if it points in flow direction.

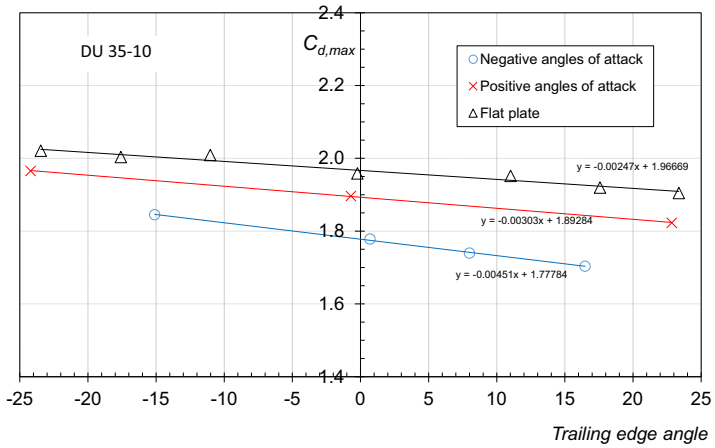

Figure 4: The maximum drag coefficients of the flat plate and of airfoil DU35-10 for various trailing edge flow angles. The flow angle is positive when the TE points downstream.

Probably due to more vibrations the flat plate measurements show more variation around the trend line. The other models are much stiffer, despite the "hat"-stiffener that was attached to the back of the plate. The 1 mm step between the flap and the airfoil surface was smoothed out with aluminium tape. Account was made for the change in angle of attack of the model with flap deflection, as the trailing edge moves away from its original chord position, which also causes small changes in the

length of the longest chord of the airfoil. As can be deduced from figure 4, the effect of a TE-angle on the maximum drag coefficient is not constant for all leading edge thicknesses. It appears that the thicker the leading edge of the airfoil the larger the impact of a trailing edge angle. Figure 5 shows this "sensitivity" to changes in the TE-angle in relation to the leading edge y/c.

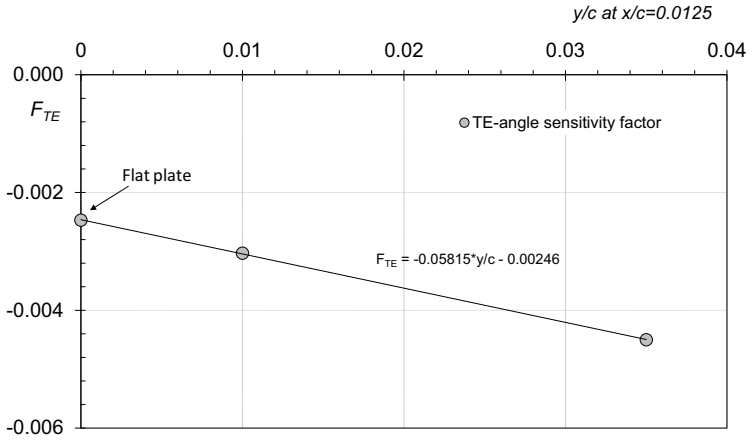

Figure 5: The variation of the sensitivity of the airfoil maximum drag to changes in the TE-flow angle with airfoil leading edge thickness

The sensitivity factor is found to be :

$$F_{TE} = -0.00246 - 0.05815 * (y/c)_{x/c=0.0125} \quad (3)$$

This sensitivity increase with LE-thickness can be explained from the fact that the circulation due to a different TE-angle changes, also changing the adverse pressure gradients at the leading edge. On a thick leading edge the flow can stay attached much longer and variation in the pressure gradients at the nose may cause changes in the separation point, leading to variations in the drag coefficient. The leading edge of a flat plate does not allow for a change in separation location; it is so sharp that this leads to immediate separation, no matter what change in circulation may exist. The contribution of the TE-angle to $C_{d,max}$ of an airfoil with specific y/c is: $F_{TE}*\zeta$.

4 Prediction of the maximum drag coefficient of various airfoils

The relations discussed above enable us to predict the maximum drag coefficient of the airfoils tested simply on the basis of their geometrical appearance. If the formulation is also suited to predict the $C_{d,max}$ of other airfoils will be discussed below.

4.1 Results found in the public domain.

As already mentioned in the introduction, many variables play a role in the results of measurement campaigns at high angles of attack found in literature. Apart from the wind tunnel wall correction scheme, insight in the suitability of which progressed with time, two equally important aspects play a paramount role.

The first is the test setup. To utilize the height of large test sections often inserts are used. In combination with a relatively small chord of a model spanning the inserts a fairly small blockage

parameter c/h can be reached. Also there is no need to manufacture a model with a large span, which saves costs and mitigates problems of model stiffness. However, complications arise when the model is set to very high angles of attack, thus only blocking the middle part of the large test section. The flow will partly avoid this blockage, which increases the velocity in the other parts of the passage. The consequence is that the flow speed between the inserts will increase due to the blockage, but not to the degree found in a test section with uniform blockage.

Here enters the importance of the second parameter, the determination of the free-stream dynamic pressure. When done with a pitot-static tube the location plays a dominant role. If it is somewhere far upstream the test section formed by the inserts, or a calibration using pressure orifices in the contraction upstream in a wider area of the tunnel channel is used, generally the lift and drag characteristics are too low, resulting from an assumed –but not realized- velocity increase over the model based on uniform blockage. In this situation the characteristics of the model can be recalculated as will be shown in paragraph 4.2. If the tube is located between the inserts upstream of the model it may be too close, as the static pressure field of the model, especially at large angles, will affect the static pressure reading of the pitot-static tube. This usually leads to smaller recorded dynamic pressures than representative for the free-stream and will cause force coefficients being too high. As it is generally unknown to what extent the static pressure is affected the latter measurements will be rather difficult to re-correct.

Unfortunately quite a number of tests found in the public domain contain measurements at high angles of attack in test sections with inserts. Table 2 gives an overview of the most relevant ones.

Table 2: *Reports containing data of test campaigns at high angles of attack using test section inserts*

Authors	Airfoil	c/h	Correction scheme	Remarks
Michos et al. [4]	NACA 0012	0.257	Maskell, θ=0.96	Rather large c/h for the present study. Dynamic pressure at entrance of t.s, but corrected (2%)
Bloy and Roberts [6]	NACA 63-215	0.138	Maskell, θ=0.96	Small model aspect ratio (2.5). Distance to pitot tube is 2.5 chords
Satran and Snyder [5]	LS(1)-0413, LS(1)-0417	0.166	for low angles	Virginia Tech University (VTU) 2.13 m x3.05 m wind tunnel,
Sheldahl and Klimas [3]	NACA 0009, 0012, 0015	0.071	not given	VTU 2.13 m x 3.05 m wind tunnel, pitot in test section
Snyder et al. [14]	NACA 23018, 24 and 30	0.107	not given	VTU 2.13 m x 3.05 m wind tunnel
	NACA 64-618			
Massini et al. [2]	Various, e.g. NACA 0012	0.135	Maskell	Correction using base pressure. Circular test section, pitot at 6.6 chords from model Uncorrected values available

Due to the uncertainties associated with the usage of test section inserts unfortunately none of the data sets from measurement campaigns mentioned in table 2 can be directly used with sufficient confidence in the reported drag values. Even the uncorrected data of Massini et al. for NACA 0012 when corrected with Maskell's method returns a near flat plate $C_{d,max}$ value of 1.995. Other data also often referred to are shown in table 3.

Table 3: *Reports containing data of test campaigns at high angles of attack using the entire test section*

Authors	Airfoil	c/h	Correction scheme	Remarks
Ostowari and Naik [7]	NACA 4409, 12, 15 and 18	0.1		Texas A&M 2.13 m x 3.05 m wind tunnel. Wooden models
Critzos et al. [1]	NACA 0012	0.067		Langley LTPT 0.914 m x 2.134 m wind tunnel. Gimball arrangement. Uncorrected data available
	NACA 0012	0.1		Langley 2.13 m x 3.05 m wind tunnel. Uncorred data available

The two references mentioned in table 3 do not give specific correction schemes, although Ostowari and Naik (and also Sheldahl and Klimas and Snyder et al.) refer to Pope and Harper [15], which classic book does not contain explicit high angle of attack correction methods. Their maximum drag coefficients are higher than 2, which points in the direction of a free-stream dynamic pressure offset. The LTPT measurements of Critzos et al. were performed using a gimball arrangement at one end of the model, while the other end was attached to a balance. With such a setup *approximately* half the load is measured, which may have affected the accuracy of the force measurement.

4.2 Re-correction of data

As the report of Satran and Snyder implicitly gives the applied correction formulae, which only apply to relatively low angles, it is possible to use Maskell's method after un-correcting the available data. The following drag correction equation was applied to un-correct the drag data:

$$C_d = C_{d_u}\left[1 - 2\Lambda\sigma - 2\tau C_{d_u}\right] \tag{4}$$

with $\Lambda = 1.75*\left(\frac{t}{c}\right) + 1.875*\left(\frac{t}{c}\right)^2$, $\sigma = \frac{\pi^2}{48}\left(\frac{c}{h}\right)^2$ and $\tau = \frac{1}{4}\left(\frac{c}{h}\right)$ (5)

where t/c is the relative thickness of the airfoil and the index u denotes uncorrected values. After a few iterations the uncorrected drag coefficient can be determined. The dynamic pressure ratio was then calculated using equation 1 assuming the passage between the inserts is the test section. However, as the velocity increase is spread over the entire test section with area 5.678 m^2 (assuming the inserts are 15 cm thick) and not only occurs in the middle passage (A=1.951 m^2) only about one third of the velocity increase (0.3436) is realized at the model location. The new dynamic pressure ratio for correction is given by equation 6:

$$\frac{q_{cor}}{q_u} = \left[1 + \left(\sqrt{\frac{q_M}{q_u}} - 1\right) * 0.3436\right]^2 \tag{6}$$

where the index M refers to Maskell's method for the test section formed by the inserts. The measurements at a Reynolds number of approximately $0.7x10^6$ from references [3] and [5] were re-corrected accordingly. The data from [14] were not fully processed as it is unclear what correction equations were used. A tentative estimate of the differences between the predicted and measured reference [14] data corrected using the procedure described above is between + and - 5%.

4.3 The effect of the Reynolds number.

As the base pressure at the downwind side of an airfoil with a smooth surface generally is reached through laminar separation at the leading edge, there will be an effect of the Reynolds number. With a higher Reynolds number the boundary layer is able to stay attached a little longer and will speed up as it rounds the LE, resulting in a lower static pressure in the separated region. This is clearly shown

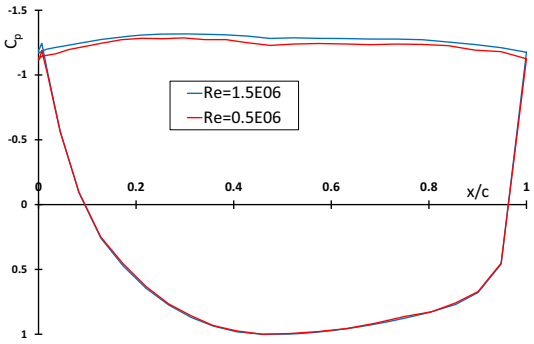

Figure 6: The corrected pressure distributions of airfoil DU 00-W-212 at 90 degrees angle of attack for two different Reynolds numbers. Uncorrected data from [16].

in figure 6, where the measured pressure distributions of airfoil DU 00-W-212 are presented at 90° angle of attack for two different Reynolds numbers.

The uncorrected data from [16] were corrected using equation 1. The lower base pressure for Re=1.5x10^6 raises the corrected maximum drag coefficient from 1.8540 at Re=0.5x10^6 to 1.8855, an increase of 1.7 %. For the higher y/c of the upper surface leading edge at negative angles this difference is 2.2 %. Since we deal with laminar separation, the turbulence intensity of the incoming flow has a comparable effect. The Reynolds number in the present study is relatively low, in the order of 0.5x10^6. This places the predicted values for the maximum drag coefficient at the lower boundary, although differences for significantly higher Reynolds numbers are only a few percent.

4.4 Comparison of predictions with measurements.

All the maximum drag coefficients presented here have been determined with a 6th degree polynomial through the drag coefficients in a range of approximately 90 degrees around -90° or 90° angle of attack. The Reynolds number ranges from 0.6x10^6 to about 0.75x10^6. Table 4 shows the

Table 4: Measured and predicted $C_{d,max}$ for airfoils tested in the Delft LTT

Airfoil	y/c	ζ	$C_{d,max}$		
Positive angles		deg.	measured	predicted	diff (%)
Flat plate	0	0	2.013	1.976	-1.8
DU 96-W-180	0.01533	-0.11	1.891	1.894	0.2
DU 91-W2-250	0.03100	-10.23	1.859	1.853	-0.3
DU 97-W-300	0.03327	-15.44	1.831	1.865	1.9
NACA 0018 *	0.02841	11.85	1.800	1.774	-1.4
Negative angles					
DU 96-W-180	0.02072	13.27	1.790	1.816	1.5
DU 97-W-300	0.03069	12.65	1.781	1.757	-1.3

predicted and measured maximum drag coefficients for a number of airfoils tested in the Delft low-turbulence tunnel. NACA 0018 and DU 91 results are yet unpublished data. DU 96 and DU 97 results come from [8]. The c/h value for the NACA 0018 test was 0.217. The trailing edge angle was calculated from the upper or lower surface dy/dx gradient at the trailing edge calculated from a 4th degree polynomial through coordinates of approximately the last 4% of the airfoil contour described by 200 coordinates. All the tests in table 4 were performed using the same force balance system. The comparison of measured and predicted values shows differences of roughly ± 1.9% with an average

Tabel 5: Measured and predicted $C_{d,max}$ for various other airfoils

Airfoil	y/c	ζ	$C_{d,max}$		
Positive angles		deg.	measured	predicted	diff (%)
LS(1)-0413	0.01531	-10.58	1.941	1.929	-0.6
LS(1)-0417	0.02129	-9.92	1.914	1.898	-0.8
NACA 63-215	0.01793	3.47	1.960	1.867	-4.7
NACA 0009	0.01894	6.00	1.867	1.880	0.7
NACA 0012 [1]	0.02072	7.99	1.859	1.846	-0.7
NACA 0012 [3]	0.02072	7.99	1.837	1.846	0.5
NACA 0015	0.02841	9.94	1.822	1.811	-0.6
DU 00-W-212	0.01756	-1.26	1.861	1.886	1.3
Negative angles					
LS(1)-0413	0.03069	14.38	1.830	1.790	-2.2
LS(1)-0417	0.03011	14.92	1.765	1.749	-0.9
DU 00-W-212	0.02142	13.39	1.771	1.811	2.3

of -0.2%. Table 5 presents the prediction of the maximum drag coefficient for various other airfoils. The NACA 63-215 $C_{d,max}$ value originates from a test using inserts with a pitot-static tube about 2.5

chords upstream of the model. The NACA 0012 value from Critzos et al. [1] was determined using Maskell's correction on uncorrected data from the NASA Langley 2.13 x 3.05 m wind tunnel. The differences amount to about ± 2.3 % with an average of -0.1%. Tables 4 and 5 are graphically

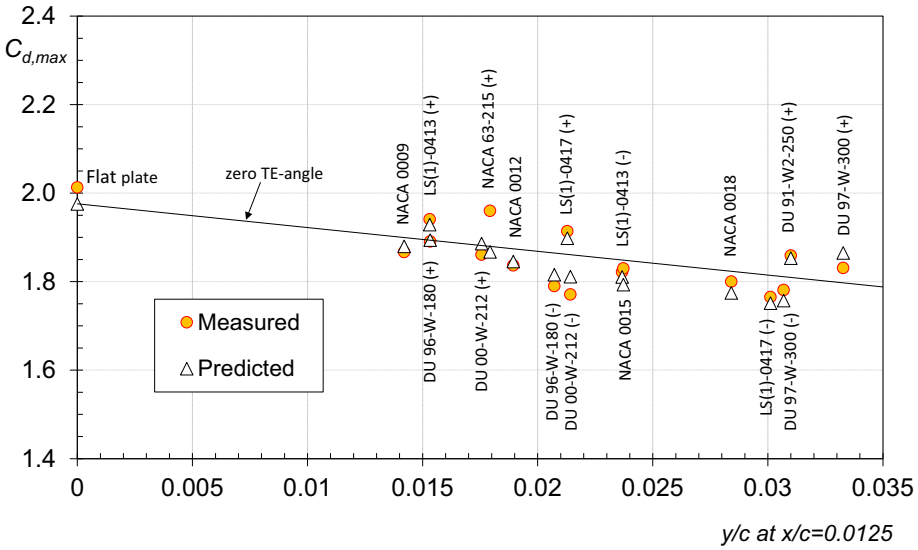

Figure 7: The measured and predicted maximum drag coefficients from tables 4 and 5. Plusses and minuses denote positive and negative angles of attack.

presented in figure 7.

5. Conclusion

A method is presented to predict the maximum drag coefficient of airfoils on the basis of measurements in the TUDelft low-speed low-turbulence wind tunnel. The method calculates a contribution due to the airfoil leading edge thickness in terms of the upwind y/c-coordinate at x/c=0.0125 using airfoil models with varying leading edge thickness and zero trailing edge angle. The contribution of the trailing edge combines the flow angle at the trailing edge with a sensitivity factor related to the afore mentioned y/c coordinate. Comparison with measured airfoil maximum drag coefficients found in the public domain gives differences up to 2.3% with an average of about -0.2%

6. References

[1] C.C. Critzos, H.H. Heyson, R.W. Boswinkle Jr. "Aerodynamic characteristics of NACA 0012 airfoil at angles of attack from 0 to 180 degrees". NACA TN 3361, 1955

[2] G. Massini, E. Rossi, S. D'Angelo. "Wind tunnel measurements of aerodynamic coefficients of asymmetrical airfoil sections for wind turbine blades extended to high angles of attack". *EC DG-XII Contract number: EN3W - 0018 - I, Conclusive Rapport. ENEA - Comitato Nazionale per la Ricerca e per lo Sviluppo dell'Energia Nucleare e delle Energie Alternative*, Roma.

[3] R.E. Sheldahl, P.C. Klimas. "Aerodynamic Characteristics of Seven Symmetrical Airfoil Sections Through 180-Degree Angle of Attack for Use in Aerodynamic Analysis of Vertical Axis Wind Turbines. *Report SAND80-2114, Sandia Laboratories*, Albuquerque, March 1981.

[4] A. Michos, G. Bergeles and N. Anthanassiadis, (National Technical University of Athens) "Aerodynamic characteristics of NACA 0012 airfoil in relation to wind generators". *Wind Engineering Vol. 7, No. 4 pp. 247-261*, 1983

[5] D. Satran and M.H. Snyder. "Two-dimensional tests of GA(W)-1 and GA(W)-2 airfoils at angles-of-attack from 0 to 360 degrees". *Wind Energy report no. 1*, Wind Energy Laboratory, Wichita State University, Kansas, USA, January 1977

[6] A.W. Bloy and D.G. Roberts, "Aerodynamic characteristics of the NACA 63_2-215 aerofoil for use in wind turbines", *Wind Engineering Vol. 17, No.2, 1993, pp.67-75*

[7] C. Ostowari, D. Naik, "Post Stall Studies of Untwisted Varying Aspect Ratio Blades with NACA44XX series Airfoil Sections – Part II", *Wind Engineering, Vol. 9, No. 3*, 1985

[8] W.A. Timmer. "Aerodynamic characteristics of wind turbine blade airfoils at high angles-of-attack". *Proceeding of the 3rd EWEA Conference –Torque 2010: The Science of making torque from wind.* Heraklion, Crete, Greece (2010).

[9] D.E. Gault, "A correlation of low-speed airfoil-section stalling characteristics with Reynolds number and airfoil geometry". *NACA technical note 3963*, Washington, March 1957

[10] E.C. Maskell "A theory of the blockage effects on bluff bodies and stalled wings in a closed wind tunnel. *ARC R&M vol. No 3400*, 1963

[11] H.J. Allen, W.G. Vincenti, "Wall interference in a two-dimensional wind tunnel, with consideration of the effect of compressibility." *NACA Report no. 782,* 1947.

[12] B.F.R. Ewald (ed). "Wind tunnel wall corrections". *AGARDograph 336*. North Atlantic Treaty Organization, October 1998

[13] J.E. Hackett and K.R Cooper. "Extension to Maskell's theory for blockage effects on bluff bodies in closed wind tunnels". *The Aeronautical Journal 105 pp. 409-418*, 2001

[14] M.H. Snyder, W.H. Wentz and A. Ahmed. "Two-dimensional tests of four airfoils at angles of attack from 0 to 360 degrees". *Wind Energy Reports no 16.* Wichita State University 1984

[15] A. Pope and J.J. Harper. "Low-speed wind tunnel testing". *John Wiley and Sons*, New York 1966

[16] J. Madsen and R. Hansen. Uncorrected data from the LM Windpower low-speed wind tunnel, measurement campaign 464. Lunderskov, Denmark, February 2017.